Seasonal Variations of Total Gaseous Mercury at a French Coastal Mediterranean Site

Nicolas Maruszczak[1][*][†], Sabine Castelle[1], Benoist de Vogüé[1], Joël Knoery[2], Daniel Cossa[1][‡]

[1] *IFREMER, Centre de Méditerranée, CS 20330, F-83507, La Seyne-sur-Mer, France*
[2] *IFREMER, Centre Nantes, BP 21109, F-44311, Nantes, France*

ABSTRACT

Total gaseous mercury (TGM) was continuously measured in 2009 and 2012, at a coastal site on the Mediterranean Sea (La Seyne-sur-Mer, France). Air temperature, humidity, wind speed and direction, and chemical parameters (O_3, CO, NO_x and PM_{10}) were also measured as tracers of atmospheric pollution. Average TGM concentrations did not differ between the two years, 2.20 ± 0.54 and 2.16 ± 0.60 ng m^{-3} for 2009 and 2012 respectively. Diurnal variations of TGM were observed for both years and linked to local industrial or urban activities. Furthermore, a clear seasonal trend was observed, with TGM minima in summer and maxima in winter. This seasonality is common to several air pollutants, like the result of the variation in the dispersion of pollutants in the boundary layer and higher photochemical activity in summer. The highest TGM concentrations (> 3 ng m^{-3}) were associated with air masses originating over urban and industrial areas of the Rhône Valley and local/regional anthropogenic sources. The influence of polluted air masses from these local/regional sources was confirmed by the significantly positive correlations between TGM and CO, NO_x and PM_{10}. We demonstrate that polluted air masses from nearby urban and industrial regions are an important source of TGM to Mediterranean coastal areas, rather than volatilization from the sea surface.

Keywords: Total gaseous mercury; Coastal Mediterranean site; Anthropogenic and local sources; Seasonal and daily variations.

INTRODUCTION

The atmosphere is an environmental compartment where volatile chemical contaminants reside before being deposited on soil and water surfaces. Therefore, it plays an important role in the dispersion of volatile pollutants over the Earth's surface. This is particularly the case for mercury (Hg), a toxic heavy metal widely distributed in the atmosphere in elemental and divalent volatile forms (Selin *et al.*, 2007). Hg is emitted to the atmosphere from both natural (Ferrara *et al.*, 2000b) and anthropogenic (Pirrone *et al.*, 2001) sources. Gaseous Elemental Mercury (GEM) is the predominant form

of Hg (95%) in the boundary layer with a residence time of about 6–24 months (Lamborg *et al.*, 2002; Slemr *et al.*, 2003), permitting its long range transport. GEM is subsequently oxidized to divalent mercury species (Hg(II)), including reactive gaseous oxidized mercury (GOM : $HgCl_2$, $HgBr_2$, $Hg(OH)_2$, etc.) and particulate bound Hg (PBM). GOM and PBM deposit rapidly (days-weeks) to continental surfaces and contaminate a variety of environments including soil, snow and water (Hammerschmidt *et al.*, 2006; Poissant *et al.*, 2008; Amos *et al.*, 2012).

The Hg cycle has been widely perturbed by human activities (Fitzgerald *et al.*, 2007; Lamborg *et al.*, 2014), and the anthropogenic component of Hg in the atmosphere is currently around 30% (Pirrone *et al.*, 2010). However, Hg evasion from the sea surface will still remain an important source of Hg in the atmosphere for a long period of time, because of the quantity of the Hg legacy and the size of the reservoir (Ferrara *et al.*, 2000a). In particular, the Atlantic Ocean and European seas have an influence on atmospheric Hg concentrations in the European troposphere, especially at coastal sites. For example, Kock *et al.* (2005) have compared long-term trends of atmospheric Hg concentrations at two coastal monitoring stations (Mace Head, Ireland and Zingst, Germany) and observed that, in addition to a seasonal signal, their measurements revealed northern hemispheric

---
[†] Present address, Observatoire Midi-Pyrénées, Laboratoire Géosciences Environnement Toulouse,
  CNRS/IRD/Université Paul Sabatier Toulouse III, 14 avenue Edouard Belin, 31400 Toulouse, France
[‡] Present address, ISTerre, Université J. Fourier, BP 53, F-38041, Grenoble, France

[*] Corresponding author.
  Tel.: +33 (0)5 61 33 26 07; Fax: +33 (0)5 61 33 28 88
  E-mail address: nicolas.maruszczak@get.obs-mip.fr

background values. The authors also showed that GEM concentration in Mace Head (1.72 ng m^{-3}) is 0.06 ng m^{-3} higher than those of Zingst (1.66 ng m^{-3}). This difference would probably be due to differences in local emissions from the sea surface, because no anthropogenic mercury source exists near Mace Head station. Photoreduction of dissolved Hg(II), which is the main pathway for GEM production in natural surface waters (Amyot *et al.*, 1997), is clearly at the origin of this process. Thus, coastal and oceanic sites are of great interest in observing both marine and continental atmospheric Hg dynamics. These observations are essential in calibrating regional and global Hg cycling models that can subsequently be used to simulate the impact of environmental policy scenarios on global Hg deposition. Several international programs for monitoring atmospheric Hg exist, e.g., Atmospheric Mercury network: AMNet, European Monitoring and Evaluation Program: EMEP, Global mercury Observation system: GMOS, Canadian Atmospheric Mercury Measurement Network: CAMNET). In this context, several projects have been devoted to the Mediterranean Sea over the last twenty years: (MAMCS: Mediterranean Atmospheric Mercury Cycle System, MOE: Mercury Species over Europe and MERCYMS: An Integrated Approach to Assess the Mercury Cycle in the Mediterranean Basin). The Mediterranean Sea elicits a particular interest for studying the Hg cycle, since it is a semi-enclosed basin,

under the influence of European and African continental inputs. The basin is sensitive and reactive to climatic and environmental changes (Bethoux *et al.*, 1999), which may affect Hg deposition and evasion (Durrieu de Madron *et al.*, 2011). Apart from the work by Wangberg *et al.* (2008), performed within the framework of the MERCYMS project, continuous monitoring of atmospheric Hg in the Mediterranean troposphere is lacking. The present study provides two-years of continuous measurements of total gaseous mercury (TGM) at a Northwestern Mediterranean coastal site (La Seyne-sur-Mer, France). The objective was to identify marine and continental Hg sources with the aid of several atmospheric environmental tracers (NO$_x$, CO, O$_3$, PM$_{10}$, and meteorological parameters).

METHODS

Site Description

All measurements were performed at La Seyne-sur-Mer, on the southeastern coast of France (43°6'21.06"N, 5°53' 7.78"E) (Fig. 1) and situated within 5 kilometers of Toulon city center. Toulon is a large urban area with approximately half a million inhabitants. Toulon hosts a commercial harbor and naval base with few industries, and one municipal waste incinerator situated in the urban area. All measuring instruments are 15 meters above sea level, 500 meters
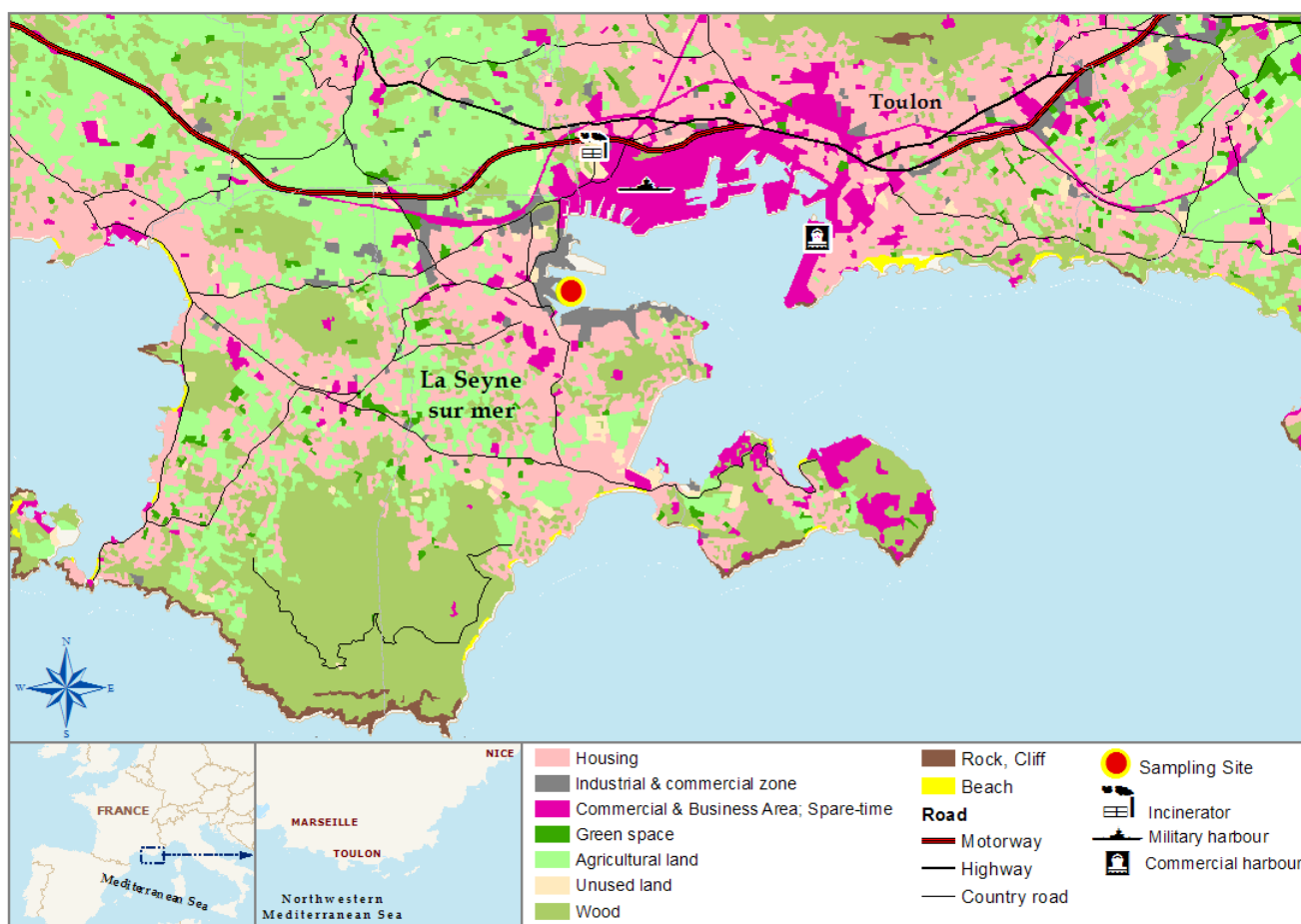

Fig. 1. Total gaseous mercury (TGM) sampling site (●) at La Seyne-sur-Mer and its local environment.

away from the closest secondary road and about 2 km from a large highway. La Seyne-sur-Mer is characterized by a Mediterranean climate: hot dry summers and mild and relatively wet winters. Winds come principally from the North-North-West or South-South-West, whereas La Seyne-sur-Mer is sheltered and protected from the North by the mountainous "massif des Maures" (780 m asl). Sometimes, there is a wind of East-South-East, often bringing rainfall. In summer, most of winds are from south (marine origin), while in winter winds come from North-North-West (continental area).

TGM Measurements

Two different analyzers have been used to measure TGM. From January 2009 to December 2009, TGM was measured directly and continuously, using a portable automated Mercury analyzer Gardis-5 (UAB Tikslioji technika, Lituania), which provides a measurement every 10 minutes. The analyzer is described in detail elsewhere (Urba *et al.*, 1995). Briefly, air is pumped through a single gold trap where atmospheric mercury is amalgamated and retained. Every 10 minutes, amalgamated mercury is desorbed and detected by cold vapor atomic absorption spectrometry (CVAAS). Ambient air (pumped at a 200 mL min^{-1} flow rate) was pre-filtered (0.45 µm pore size, LCR Millipore) to prevent the entry of particulate matter into the measurement system. The filter was changed every two weeks and instrumental sensitivity controlled daily and automatically with several injections from an external calibration unit (Model GA-730 Mercury Vapor Dosing Unit).

The second instrument was used from January to December, 2012. Measurements of TGM were carried out using a Tekran Model 2537A (Tekran Inc., Canada). The analytical technique (CVAFS) is based on the collection of ambient mercury onto two gold traps, followed by thermal desorption and final detection by cold vapor atomic fluorescence spectrometry (CVAFS). The time resolution was 5 min, the sampling flow rate was 1.5 L min^{-1} and the analyzer was self-calibrated every 47 hours by an internal Hg permeation source. A 47 mm diameter Teflon filter (pore size 0.45 µm) is placed in front of the sample line to prevent the entry of particles into the system. This filter was changed every 2 weeks. An intercomparison of these two instruments was made by Munthe *et al.* (2001) and has shown that the results are comparable (Munthe *et al.*, 2001).

Meteorological, Chemical Parameters and Statistics

Meteorological data were collected with a weather station located at La Seyne-sur-Mer, close to the sampling site. The station measured atmospheric temperature (T), air pressure (AP), and humidity (RH). Regarding wind speed (WS) and wind direction (WD) we have use the regional mesoscale model MM5 (Grell *et al.*, 1994) of the Pennsylvania State University. Different chemical parameters were also measured at La Seyne-sur-Mer (Air-PACA) including nitrogen oxides (NO_x), ozone (O_3) and particulate matter inferior at 10 µm (PM_{10}). NO_x was measured by chemiluminescence (Model 200E, Teledyne instrument), O_3 by UV absorption (Model O341M, Environnement S.A.) and PM_{10} by quartz

microbalance (Model BAM-1020, Met One Instruments). Carbon monoxide (CO) has been measured by IR absorption (Model T300U, Teledyne instrument). In order to assess the impact of meteorological parameters, three-day back-trajectories were used to identify air mass origins during the sampling period in this study. The three days backward trajectories were calculated using the NOAA HYSPLIT 4 with the EDAS (Eta Data Assimilation System) meteorological data and vertical mixing model. Arrival heights of 500 meters (m), 150 m and 15 m were used to describe the regional meteorological patterns.

All statistical analyses were carried out using JMP 10 software (SAS Institute). Correlation analysis was carried out using a correlation matrix. Statistical significance was determined for a probability of α < 0.05. A statistical summary of all chemical and meteorological parameters is presented in Table 1.

Quality Assurances and Quality Control Procedure

Both instrument have an automatic calibration step with an internal mercury permeation source for Tekran instrument and an external calibration unit (Model GA-730 Mercury Vapor Dosing Unit) for Gardis instrument. All data and all maintenance were treated by a QA/QC procedure with a software program developed by the LGGE (Laboratoire de Glaciologie et Géophysique de l'Environnement). QA/AC procedure is describe by Angot *et al.* (2014).

RESULTS AND DISCUSSION

Average Concentration and Seasonal Variations of TGM

Ambient TGM concentrations ranged from 1.15 to 5.73 ng m^{-3} (average 2.20 ± 0.54 ng m^{-3}) in 2009 and from 1.19 to 6.15 ng m^{-3} (average 2.16 ± 0.60 ng m^{-3}) in 2012. The ambient concentrations of TGM from 16th January 2009 to 31st December 2009 and from 16th January 2012 to 31st December 2012 at La Seyne-sur-Mer are shown in Fig. 2. These values are roughly 30% more elevated than the global background concentration in the Northern Hemisphere (1.75 ng m^{-3} in 1996–1999 to about 1.4 ng m^{-3} in 2009) (Lindberg *et al.*, 2007; Slemr *et al.*, 2011). High annual averages and frequent occurrence of pollution events (Fig. 2) suggest that a large proportion of the measurements are not background concentrations. These results are somewhat higher than those observed at another Mediterranean coastal site (EMEP station Cabo de Creus in Spain, Thau Lagoon in France, Piran in Slovenia, Lucido in Italia and Neve Yam in Israel) by Wängberg *et al.* (2008), with TGM observed concentrations of 1.75–1.8 ng m^{-3}, but similar to other studies at coastal sites in the world with a TGM concentration from 1.6 ng m^{-3} to 2.4 ng m^{-3} (Wangberg *et al.*, 2001) or with TGM concentration of 2.55 ng m^{-3} (Ci *et al.*, 2011). These average concentrations of TGM are higher that other TGM measurements in northern Europe (Munthe *et al.*, 2001) confirming that TGM concentrations are higher in the Mediterranean region than in the Northern Europe, where industrials and urban areas are more numerous (Pirrone *et al.*, 2001; Kotnik, 2013).

We observed a seasonal variation in TGM concentration,

Table 1. Statistical summary of all parameters (T: Temperature; WS : wind speed, WD: Wind direction; AP: Air pressure; RH: Relative humidity; O_3: Ozone; CO: Carbon monoxide; NO_x: Nitrogen oxyde; PM_{10}: particulate matter inferior at 10 μm) for both years, 2009 and 2012.

	TGM (ng m^{-3})	T (°C)	WS (m s^{-1})	WD (°N)	AP (hPa)	RH (%)	O_3 (μg m^{-3})	CO (μg m^{-3})	NO_x (μg m^{-3})	PM_{10} (μg m^{-3})
					2009					
n	5602	8399	2799	2799	8399	8399	8255	8255	8255	8389
Aveage	2.2	16.89	4.93	218.14	1013.35	69.32	28.05	386.28	28.59	28.74
Std. Dev	0.54	6.53	3.11	92.26	7.2	16.22	18.51	417.81	40.61	16.6
Min.	1.15	−1.3	0.11	0	980	15	0	0	0	0
Max.	5.73	34.5	16.36	360	1031	97	98.5	2707.42	460.53	124
Median	2.13	16.8	4.46	211	1015	72	28.5	174.67	15.43	26
					2012					
n	7933	8037	2791	2791	8037	8165	8376	750	8374	7725
Aveage	2.16	17.38	4.82	221.14	1013.5	66.48	28.7	607.21	29.08	30.2
Std. Dev	0.6	7.06	3.2	92.02	18.22	15.07	16.36	160.13	44.04	17.79
Min.	1.19	−2.2	0.1	0	916	23	0	478.8	0	0
Max.	6.16	36.3	21.1	360	1033	94	91.5	1847.8	463.76	139
Median	2.02	17.4	4.2	216	1018	67	29.5	546.62	14.63	29

with a maximum of 2.51 ± 0.44 ng m^{-3} in winter (Dec–Feb) and minimum of 1.95 ± 0.53 ng m^{-3} in summer (Jun–Aug) for 2009 and a maximum of 2.43 ± 0.72 ng m^{-3} in winter and a minimum of 1.97 ± 0.57 ng m^{-3} in autumn (Sept–Nov) for 2012 (Fig. 3). The influence of different meteorological and atmospheric chemical parameters on TGM concentrations for each season and each year were investigated. A multivariate analysis (Table 2) shows that TGM concentrations were negatively correlated with wind speed factor for each season of each year (2009: winter r = –0.39; spring, r = –0.04; summer, r = –0.25; fall, r = –0.17. 2012: winter r = –0.41; spring, r = –0.19; summer, r = –0.29; fall, r = –0.43). This suggests that the seasonal TGM concentration observed at La Seyne-sur-Mer are not due to TGM inputs from wind transport of terrestrial or marine origin but a local production of TGM. This statement was verified by analyzing the influence of atmospheric chemical parameters (CO, O_3, NO_x and PM_{10}) for each season. However, it is possible that with a high wind speed, mixing of air masses is greater, and thus a dilution of TGM and other pollutant within the boundary layer. Furthermore, the multivariate analysis (Table 2) shows that for each season of both years, TGM concentrations were significantly correlated with other chemical parameters. This seasonal phenomenon is common to several air pollutants and explained as the result of the dispersion of pollutants in the boundary layer, due to changes in air mass stratification with temperature. The atmospheric boundary layer is thicker in summer due to greater solar radiation, which promotes convection, and, thus, a better dispersion of Hg in thicker atmospheric layers. In addition, we observe a significant positive correlation between TGM and CO in winter for both year (r = 0.16; p < 0.0001 for 2009 and r = 0.46; p < 0.0001 for 2012), and it is known that domestic heating using the combustion of fossil fuels, can intensify atmospheric emissions during

winter (CO and TGM), when the atmospheric mixing layer is thinner (Kock *et al.*, 2005). If we compare seasonal TGM and O_3 variations, we observe a significant negative correlation for each season of each year (2009: winter r = –0.54; spring, r = –0.32; summer, r = –0.34; fall, r = –0.44. 2012: winter r = –0.42; spring, r = –0.44; summer, r = –0.53; fall, r = –0.58). Indeed, O_3 is maximal in summer and minimal in winter, while TGM is minimal in summer and maximal in winter. It is known that the tropospheric ozone concentrations are higher in summer than in winter, due to a stronger solar radiation and thus a higher O_3 production in the summer. Indeed, tropospheric ozone is formed primarily by photochemical reactions involving pollutants emitted by human activities, including nitrogen oxides (NO_x) and volatile organic compounds (VOCs). A high O_3 concentration reflects a strong atmospheric oxidant potential. A strong atmospheric oxidant potential can cause a possible higher GEM oxidation to GOM by radical •OH or halogens compounds (Br, BrO), which is rapidly deposited and seen in the decrease in TGM. Thereby TGM concentration may decrease in summer due to a strong potential atmospheric oxidation between GEM and GOM.

An another explanation to confirm this TGM seasonality, is the fact that is exist a seasonal variation of the origin of air masses which arrive at La Seyne-sur-Mer, and generally in this part of coastal Mediterranean. Indeed, in summer the majority of air masses have a marine origin (South South–Est), while in winter the air masses come essentially from north north–west, with a continental origin. As well, a marine air mass is less contaminated in mercury than a continental air mass. Indeed, Kotnik *et al.* (2013) show that the TGM concentration over the Mediterranean Sea is lower (1.6–1.9 ng m^{-3}) than TGM measurements at La Seyne-sur-Mer. This observation and this correlation could explain also this seasonal variation. This situation is opposite
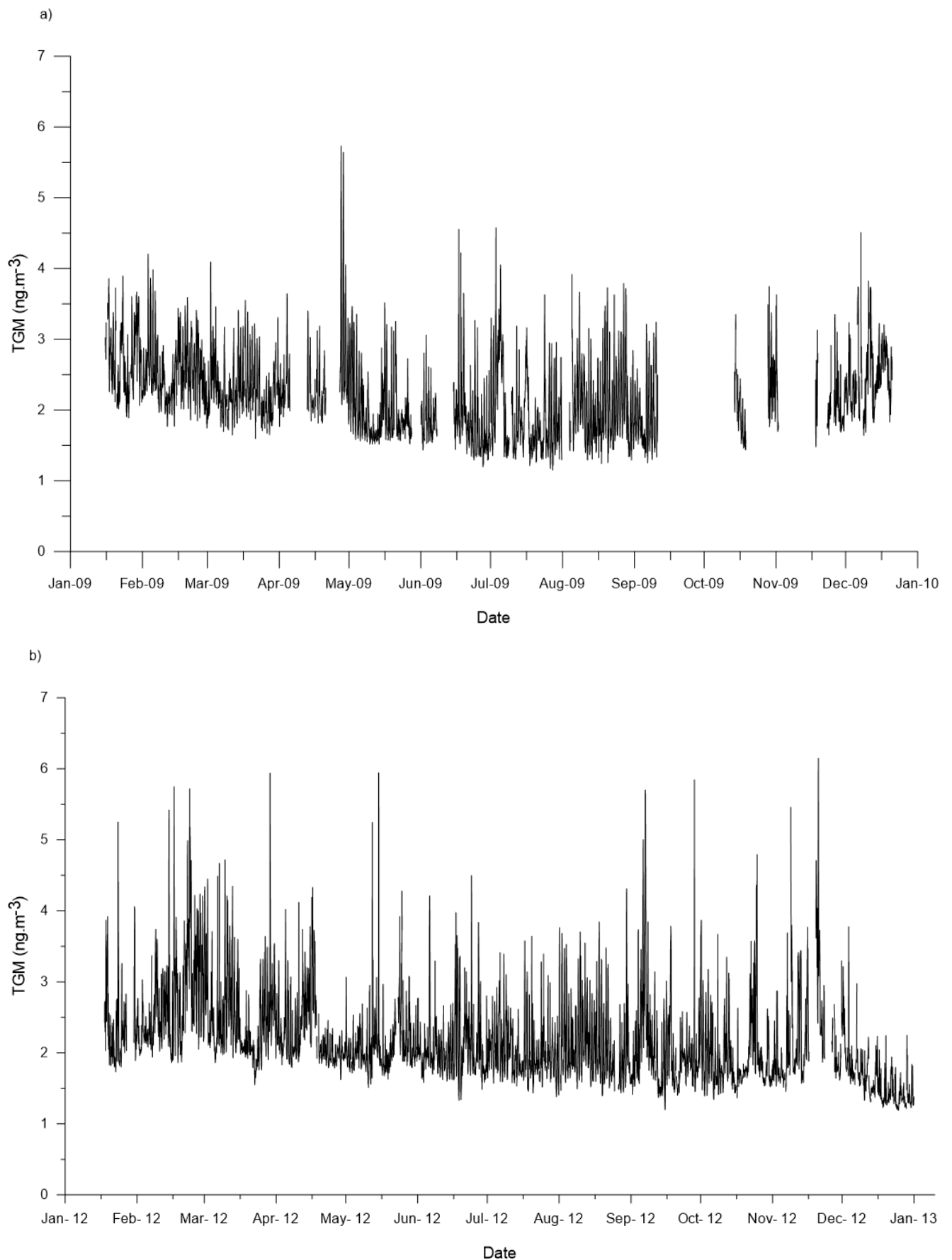
a)

b)

Fig. 2. TGM concentrations (hourly mean) measured at La Seyne-sur-Mer in 2009 (a) and 2012 (b).
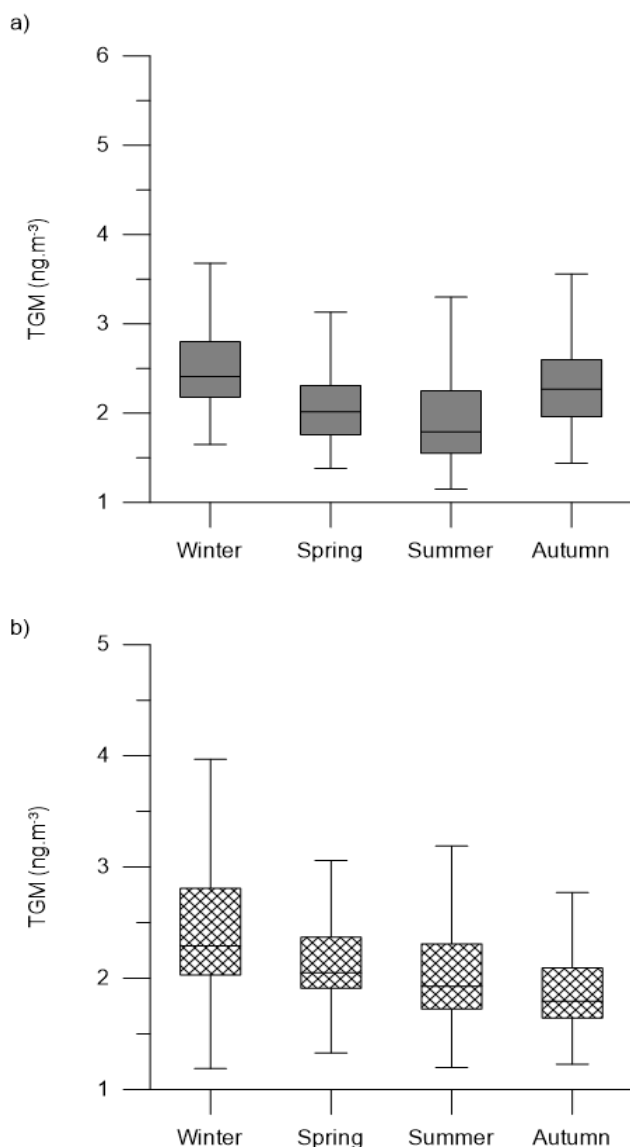
a)

b)

Fig. 3. Box and whisker plot of the average seasonally of TGM at La Seyne-sur-Mer in 2009 (a) and 2012 (b). Boxes extend from 25 to 75% quartiles; the middle line represents the median value. The whiskers extend from Min to Max values.

from that described in Wängberg *et al.* (2008). They compared atmospheric Hg concentrations at five other coastal Mediterranean sites, and observed an opposite seasonal cycle with maxima in summer and minima in winter. They attributed these variations to TGM evasion from the sea surface. Their measurements were conducted during 4 field campaigns of 15 days each season. We can infer from these diverging observations that local and regional atmospheric conditions are able to generate various types of seasonality in the TGM atmospheric signal. La Seyne-sur-Mer and more generally the urban area of Toulon, with numerous activities (naval and tourist port, militaries activity) play a strong role in the TGM concentration with a seasonal patterns primarily due to the anthropogenic activities of the urban area.

Daily Variations of TGM.

Fig. 4 illustrates the daily variation in TGM at La Seyne-sur-Mer for 2012, averaged over both monitoring years. TGM maxima occur in the early morning and minima in the middle of the afternoon during all seasons. Two hypotheses can be put forward to explain these daily TGM variations: (i) daily solar radiation variation, inducing a daily cycle in the amplitude of the photoreduction of Hg(II) from surface waters and soils; and/or (ii) the daily cycle of the urban or industrial activities around the observation site. At La Seyne-sur-Mer for daily-averaged observations, covariations of TGM and other monitored atmospheric pollutants are observed. For example, Fig. 5 shows the variation of TGM, O_3, NO_x, CO and PM_{10} in December 2012. We observed that TGM, NO_x, CO and PM_{10}, exhibit the same pattern during December 2012. Most of observed increases of CO, NO_x, PM_{10} and TGM occur together, from the middle of afternoon to noon the next day (4:00 pm to 12:00 pm). This observation reflected that TGM is directly in relationship with these anthropogenic pollutants. These pollutants are essentially produced by motor traffic (NO_x) and fossil fuel combustion (CO, and PM_{10}) and are considered as tracers of local pollution. O_3 also is affected by the high concentration of NO_x as NO oxidation consumes, and thereby lowers, O_3 to produce NO_2. The diurnal variation of TGM can thus be affected by the combination of local chemical reaction, natural/anthropogenic sources, mixing height variation, and transport. Also, the combustion of fossil fuel (for domestic heating) could increase the concentration of TGM, NO_x and other compounds in the atmosphere. For example, from 11th December 2012 at 4:00 p.m. to 12th December at 3:00 p.m., mercury concentrations increased progressively and strongly to a maximum of 2.22 ng m^{-3} at 9:00 a.m. Conversely, the atmospheric temperature has experienced a sharp decline to reach 1.3°C on 12th December at 4:00 a.m. However, it is highly likely that with these temperatures, the consumption of fossil fuels for domestic heating has increased. This results in a net increase in the concentrations of CO and PM_{10} that are two tracers of anthropogenic and local emissions. Thus, it appears that the daily variations of TGM during this period are principally due to the cyclic activity of urban and industrial activities near the sampling site. The hypothesis of a natural origin for the daily variations is not supported by our results. While a marine origin of TGM cannot be ruled out, we suggest that in coastal regions impacted by industrial and urban areas, anthropogenic Hg emissions may be the main factor controlling the daily variations in TGM concentrations.

Air Masses Affecting TGM Concentrations

To improve the insights and understanding of TGM concentrations measured at La Seyne-sur-Mer, we analyzed correlations between meteorological parameters (wind direction, wind speed, humidity, dew point and temperature) and TGM concentrations. The wind directions presented in Figs. 6(a) and 6(b) show that at La Seyne-sur-Mer most winds came from North-North-West and South-South-West for both years. These wind directions show that the majority of the air masses passing over the sampling site in 2009 and

Table 2a. Multivariate analysis of all parameters (T: Temperature; WS : wind speed, WD: Wind direction; AP: Air pressure; RH: Relative humidity; O₃: Ozone; CO: Carbon monoxide; NOx: Nitrogen oxyde; PM₁₀: particulate matter inferior at 10 μm) for each season of 2009. Values statistically significant (α < 0.05) are shown with an asterisks.

Fall

	TGM	T	WS	WD	AP	RH	O₃	CO	NOx	PM₁₀
TGM	1.00*									
T	-0.34*	1.00*								
WS	-0.17*	-0.33*	1.00*							
WD	0.06	-0.41*	0.33*	1.00*						
AP	-0.07	0.48*	-0.42*	-0.33*	1.00*					
RH	0.07*	0.10*	-0.23*	-0.15*	0.23*	1.00*				
O₃	-0.44*	0.44*	0.12*	-0.21*	0.00	-0.19*	1.00*			
CO	0.24*	0.12*	-0.34*	-0.14*	0.15*	0.01	-0.19*	1.00*		
NOx	0.40*	-0.12*	-0.29*	-0.04	0.14*	0.08*	-0.56*	0.53*	1.00*	
PM₁₀	0.37*	0.26*	-0.49*	-0.23*	0.49*	0.27*	-0.29*	0.41*	0.51*	1.00*

Spring

	TGM	T	WS	WD	AP	RH	O₃	CO	NOx	PM₁₀
TGM	1.00*									
T	-0.16*	1.00*								
WS	-0.04	-0.15*	1.00*							
WD	0.04	-0.28*	0.29*	1.00*						
AP	-0.11*	0.20*	-0.27*	-0.20*	1.00*					
RH	0.00	-0.48*	-0.21*	0.04	-0.06*	1.00*				
O₃	-0.32*	0.46*	0.19*	-0.27*	-0.05*	-0.36*	1.00*			
CO	0.06*	0.42*	-0.19*	-0.11*	0.07*	-0.09*	-0.07*	1.00*		
NOx	0.29*	-0.16*	-0.16*	0.05*	0.09*	0.08*	-0.63*	0.33*	1.00*	
PM₁₀	0.09*	0.22*	-0.14*	-0.14*	0.19*	0.04*	-0.08*	0.24*	0.38*	1.00*

Winter

	TGM	T	WS	WD	AP	RH	O₃	CO	NOx	PM₁₀
TGM	1.00*									
T	0.00*	1.00*								
WS	-0.39*	-0.14*	1.00*							
WD	-0.32*	-0.23*	0.36*	1.00*						
AP	0.00*	0.00	-0.39*	0.00	1.00*					
RH	0.31*	-0.02	-0.27*	-0.34*	-0.23*	1.00*				
O₃	-0.54*	0.41*	0.29*	0.09	0.00	-0.35*	1.00*			
CO	0.41*	-0.21*	-0.31*	-0.11*	0.13*	0.25*	-0.62*	1.00*		
NOx	0.46*	-0.23*	-0.31*	-0.09	0.17*	0.15*	-0.60*	0.86*	1.00*	
PM₁₀	0.44*	-0.04	-0.51*	-0.17*	0.40*	0.20*	-0.41*	0.58*	0.57*	1.00*

Summer

	TGM	T	WS	WD	AP	RH	O₃	CO	NOx	PM₁₀
TGM	1.00*									
T	0.03*	1.00*								
WS	-0.25*	-0.02	1.00*							
WD	-0.13*	-0.29*	0.41*	1.00*						
AP	0.03	0.01	-0.27*	-0.20*	1.00*					
RH	0.19*	-0.41*	-0.48*	-0.15*	0.10*	1.00*				
O₃	-0.34*	0.57*	0.06	-0.27*	-0.16*	-0.16*	1.00*			
CO	0.15*	0.14*	-0.27*	-0.17*	0.05*	-0.04	-0.11*	1.00*		
NOx	0.41*	-0.14*	-0.16*	-0.03	0.18*	0.04	-0.55*	0.35*	1.00*	
PM₁₀	0.21*	0.38*	-0.20*	-0.21*	0.07*	0.11	0.16*	0.21*	0.20*	1.00*

Table 2b. Multivariate analysis of all parameters (T: Temperature; WS : wind speed, WD: Wind direction; AP: Air pressure; RH: Relative humidity; O_3: Ozone; CO: Carbon monoxide; NO_x: Nitrogen oxyde; PM_{10}: particulate matter inferior at 10 μm) for each season of 2012. Statistically significant ($\alpha < 0.05$) are shown with an asterisks. (N.D. signify No Data).

Fall

	TGM	T	WS	WD	AP	RH	O_3	CO	NO_x	PM_{10}
TGM	1.00*									
T	–0.10*	1.00*								
WS	–0.43*	–0.17*	1.00*							
WD	–0.07	–0.31*	0.25*	1.00*						
AP	0.02	0.11*	–0.13*	0.02	1.00*					
RH	0.37*	0.08*	–0.41*	–0.34*	–0.06*	1.00*				
O_3	–0.58*	0.51*	0.33*	–0.10*	0.07*	–0.36*	1.00*			
CO	0.43*	–0.17*	–0.30*	0.03*	0.74*	0.12*	–0.44*	1.00*		
NO_x	0.47*	–0.25*	–0.31*	–0.03	0.06*	0.17*	–0.58*	0.55*	1.00*	
PM_{10}	0.48*	0.19*	–0.43*	–0.20*	0.23*	0.26*	–0.26*	0.53*	0.48*	1.00*

Spring

	TGM	T	WS	WD	AP	RH	O_3	CO	NO_x	PM_{10}
GEM	1.00*									
T	–0.25*	1.00*								
WS	–0.19*	–0.26*	1.00*							
WD	0.09*	–0.30*	0.36*	1.00*						
AP	–0.27*	0.45*	–0.28*	–0.11*	1.00*					
RH	0.12*	–0.49*	–0.21*	–0.02	–0.14*	1.00*				
O_3	–0.44*	0.57*	0.15*	–0.22*	0.11*	–0.49*	1.00*			
CO	N.D.	N.D.	N.D.	N.D.	N.D.	N.D.	N.D.	N.D.		
NO_x	0.34*	–0.02	–0.21*	–0.01	0.02	0.08*	–0.43*	0.00*	1.00*	
PM_{10}	0.15*	0.36*	–0.22*	–0.19*	–0.09*	–0.01	0.09*	0.00*	0.38*	1.00*

Winter

	TGM	T	WS	WD	AP	RH	O_3	CO	NO_x	PM_{10}
TGM	1.00*									
T	–0.30*	1.00*								
WS	–0.41*	0.13*	1.00*							
WD	–0.16*	–0.11*	0.29*	1.00*						
AP	0.00	0.30*	–0.22*	–0.13*	1.00*					
RH	0.05*	–0.14*	–0.31*	–0.07	0.32*	1.00*				
O_3	–0.42*	0.48*	0.21*	–0.13*	0.00	–0.15*	1.00*			
CO	0.97*	–0.35*	–0.45*	–0.16	0.05*	0.05*	–0.49*	1.00*		
NO_x	0.39*	–0.15*	–0.24*	–0.06	0.04*	–0.15*	–0.50*	0.52*	1.00*	
PM_{10}	0.69*	–0.16	–0.43*	–0.20*	0.17*	0.10	–0.28*	0.73*	0.44*	1.00*

Summer

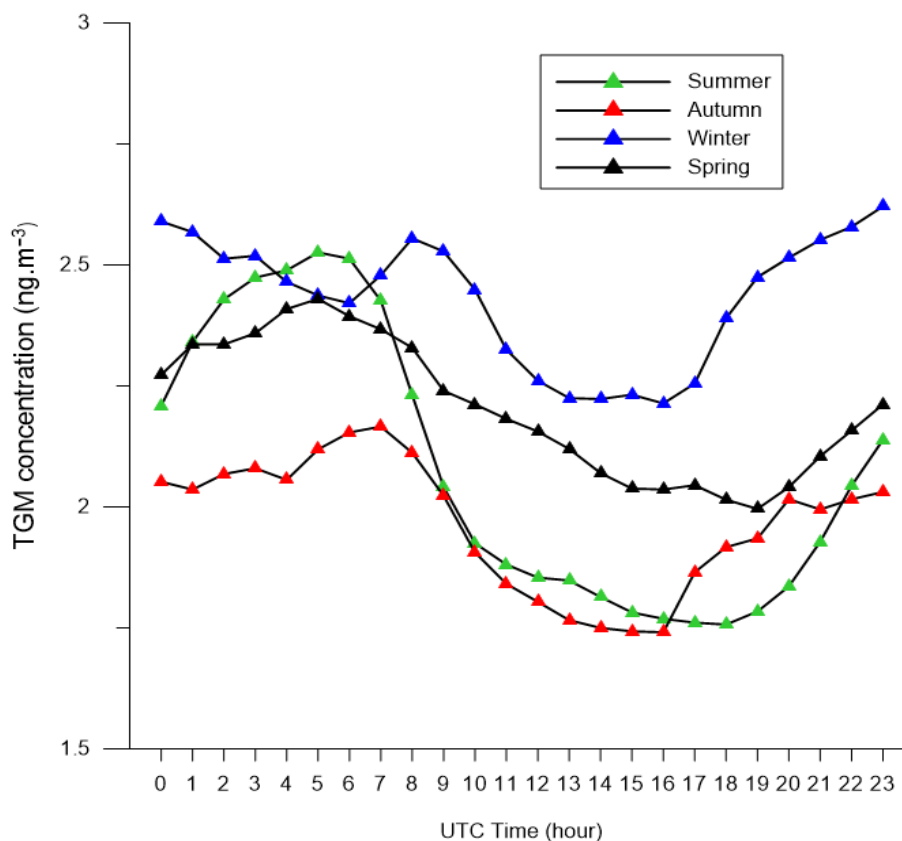|	TGM	T	WS	WD	AP	RH	O_3	CO	NO_x	PM_{10}
TGM	1.00*									
T	–0.36*	1.00*								
WS	–0.29*	–0.11*	1.00*							
WD	0.08*	–0.42*	0.40*	1.00*						
AP	0.14*	0.06*	–0.20*	–0.01	1.00*					
RH	0.41*	–0.47*	–0.31*	0.08	–0.01*	1.00*				
O_3	–0.53*	0.64*	0.08*	–0.24*	0.00	–0.50*	1.00*			
CO	N.D.	N.D.	N.D.	N.D.	N.D.	N.D.	N.D.	N.D.		
NO_x	0.34*	–0.06*	–0.31*	–0.11*	0.15*	0.06*	–0.32*	0.00*	1.00*	
PM_{10}	0.23*	0.33*	–0.29*	–0.19*	0.06*	0.12*	0.16*	0.00*	0.39*	1.00*

Fig. 4. Hourly variations of TGM by season at La Seyne-sur-Mer in 2012.

2012 have a continental imprint. In particular the air masses passing over the Marseille-Aix-en-Provence urban area, with its 1.7 million inhabitants, and those from the Rhone valley. Winds from the East were also observed for both years, and are often linked to rain events in the area.

Multivariate correlation analysis (Table 2) shows that TGM is not significantly correlated with wind direction (r = –0.02; p = 0.4603 for 2009 and r = 0.15; p < 0.0209 for 2012) but a significant negative correlation between wind speed and TGM exists (r = –0.08; p = 0.0005 for 2009 and r = –0.37; p < 0.0001 for 2012). These observations confirm that a local production of TGM is predominant, compared to a long range transport of TGM. However, if we consider high concentrations of TGM (> 3 ng m^{-3}), Fig. 7 shows that they were predominantly observed with a light breeze from West-South-West sector for both years and with an average of wind speed of 3.5 m s^{-1} for 2009 and 3.2 m s^{-1} for 2012. These averages of wind speed correspond to a Beaufort class of 2, so a light breeze. This confirms that all TGM concentration superior at 3 ng m^{-3} come from probably of a local production by industries or urban area. However, we observe that concentrations of TGM superior at 3 ng m^{-3} coming from West (North-West and South-West) represent 69% for 2009 and 86% for 2012 for all measurements like show by the TGM rose (Fig. 7). These sectors correspond to the "Mistral" wind. "Mistral" is a cold and strong wind coming from the Rhône Valley (North of La Seyne-sur-Mer) and then, which spreads to eastern in direction to Toulon. These air masses are very much imprinted either

by the Rhône-Valley or the Marseille-Aix urban and industrial area. Both can have a strong influence on TGM concentration, and especially because of the many anthropogenic and human activities. To verify this, we have simulated three days back trajectories (Fig. 8) with a new trajectory every 3 hours when an episode of high significant concentration of TGM (> 3 ng m^{-3}) was observed for either year (18th June 2009, 06:00 am; 05th July 2009, 06:00 am; 14th February 2012, 06:00 pm; 07th September 2012). We show that all simulated back trajectory have air masses with a continental origin and particularly imprinted by the Rhone Valley or the Marseille-Aix urban and industrial area. This observation confirms the fact that the high concentrations of TGM (> 3 ng m^{-3}) have also a continental and anthropogenic origin and are transported by these air masses. In short, we show that the highest TGM concentrations occur during (i) "Mistral" wind periods, draining the influence of anthropogenic Hg inputs from the Rhone Valley and the Marseille-Aix area and/or (ii) during the wind is very low (Beaufort Classes 2) confirming a local production of TGM. Consequently, the highest concentrations of TGM (> 3 ng m^{-3}) measured at La Seyne-sur-Mer are mainly due to industrial or urban activities and thus to regional activities.

CONCLUSIONS

This study investigated TGM concentrations at a coastal Mediterranean site (La Seyne-sur-Mer) in relation to other atmospheric pollutants (CO, O$_3$, NO$_x$ and PM$_{10}$) and
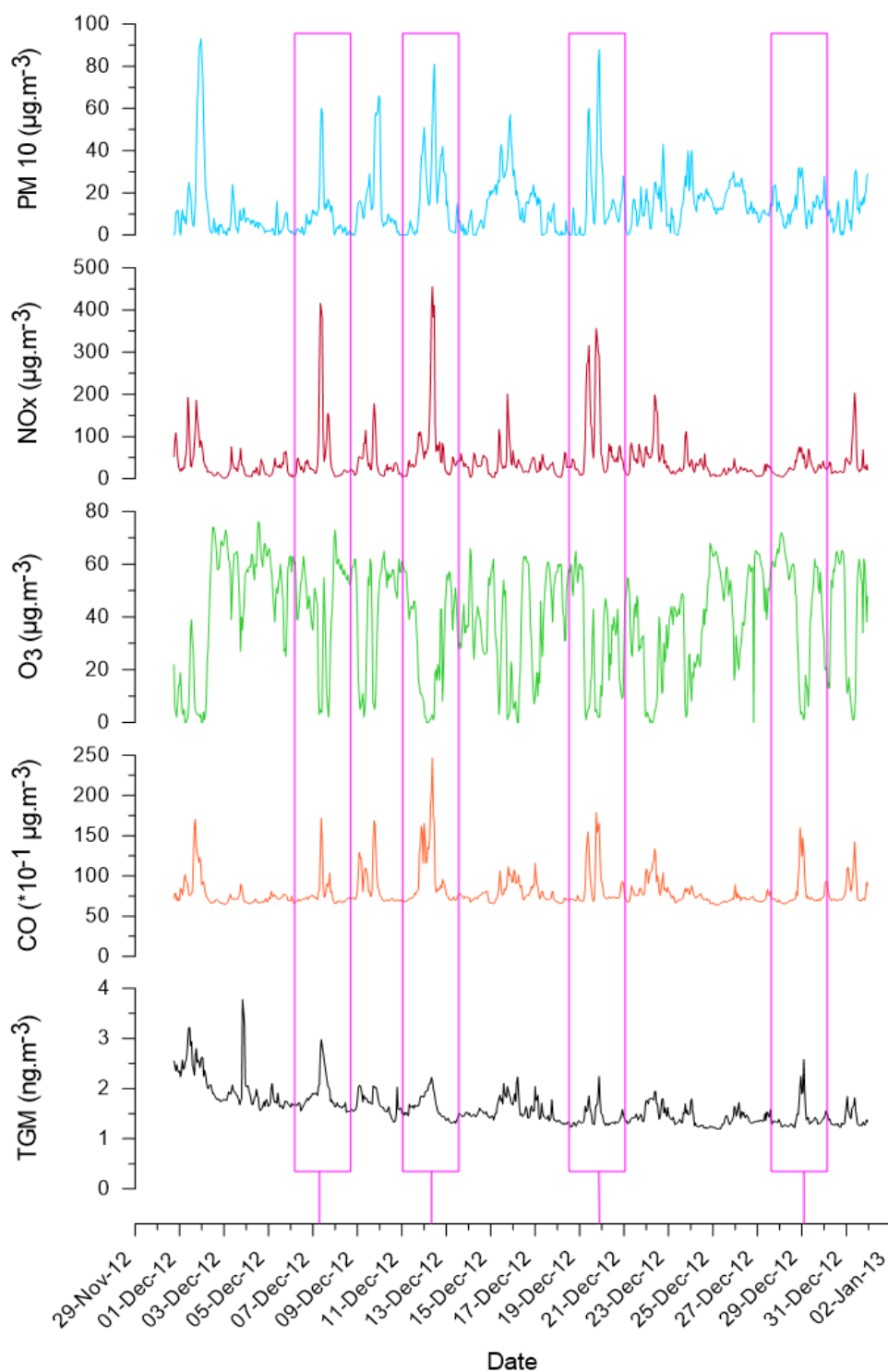
Fig. 5. Comparison of TGM and pollutants variations (PM_{10}, NO_x, O_3 and CO) during December 2012. Magenta rectangles show episodes of TGM increase in relation with the others pollutants.

meteorological parameters. We show that seasonal and daily cycles are superimposed on the regional TGM background. The seasonal variations of TGM show maximum levels in winter and minimum levels in summer, associated with the variation of other atmospheric contaminants (CO, NO_x and PM_{10}). Daily TGM variation correlates with cyclic urban and industrial activities in the area, suggesting the influence of

anthropogenic emissions even in coastal regions. This anthropogenic influence is both local (when winds are weak) and regional under the northerly wind ("Mistral") regime, which saw the highest TGM concentrations (> 3 ng m^{-3}) observed at the study site. Above a background concentration level at this coastal site, observed variations of TGM are mainly due to local and regional anthropogenic sources.

a)

b)
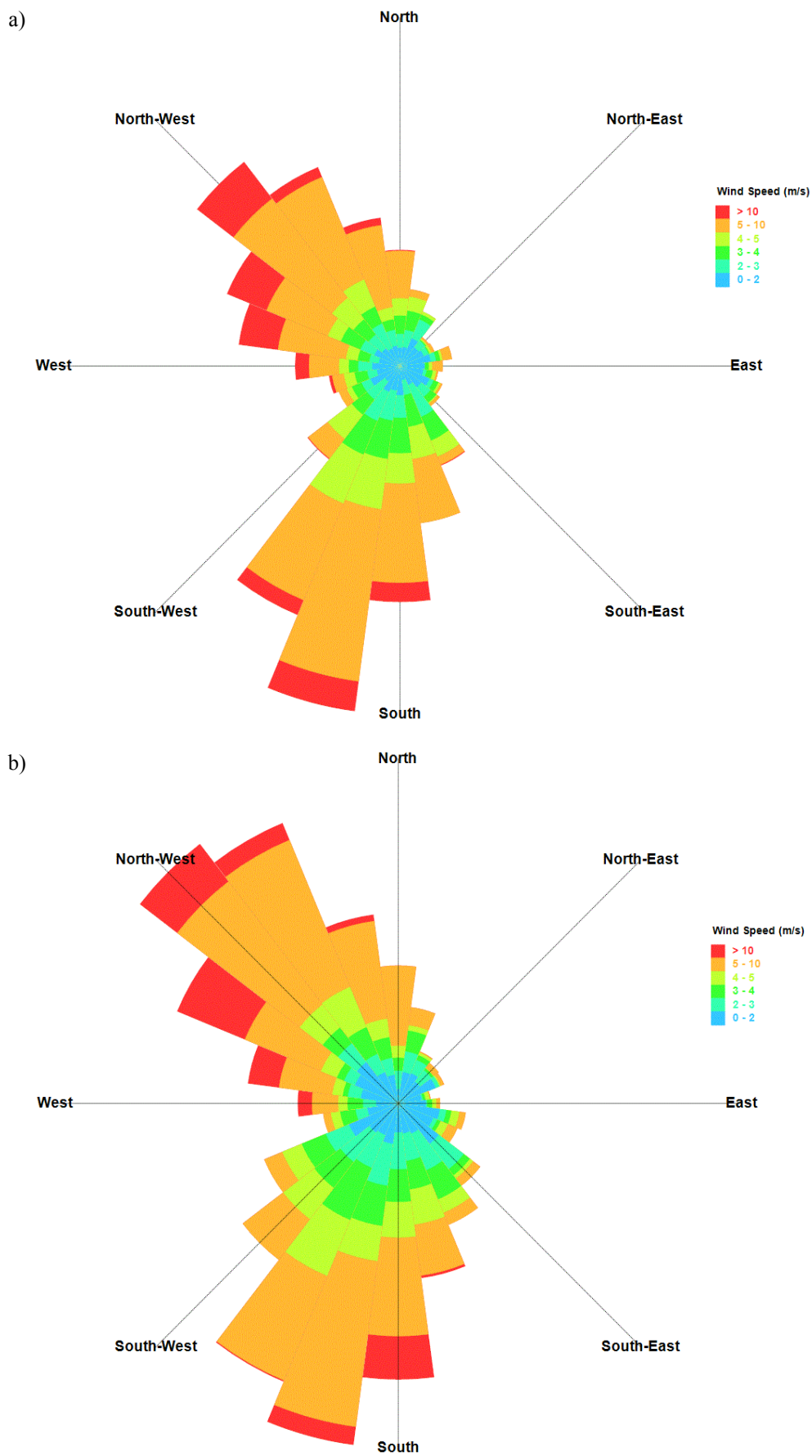
Fig. 6. Wind rose for 2009 (a) and 2012 (b).

a)

b)
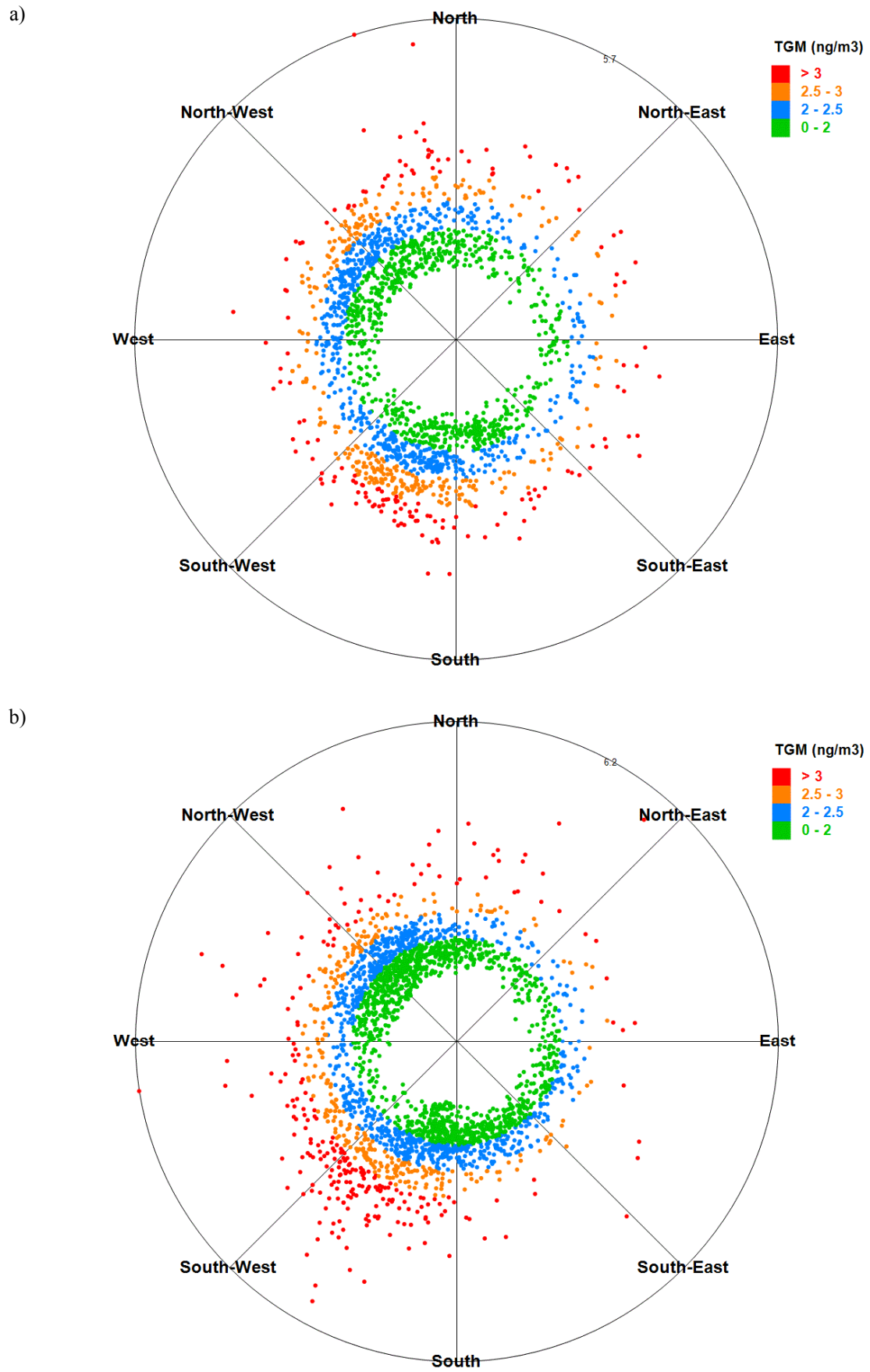
Fig. 7. TGM rose for 2009 (a) and 2012 (b).
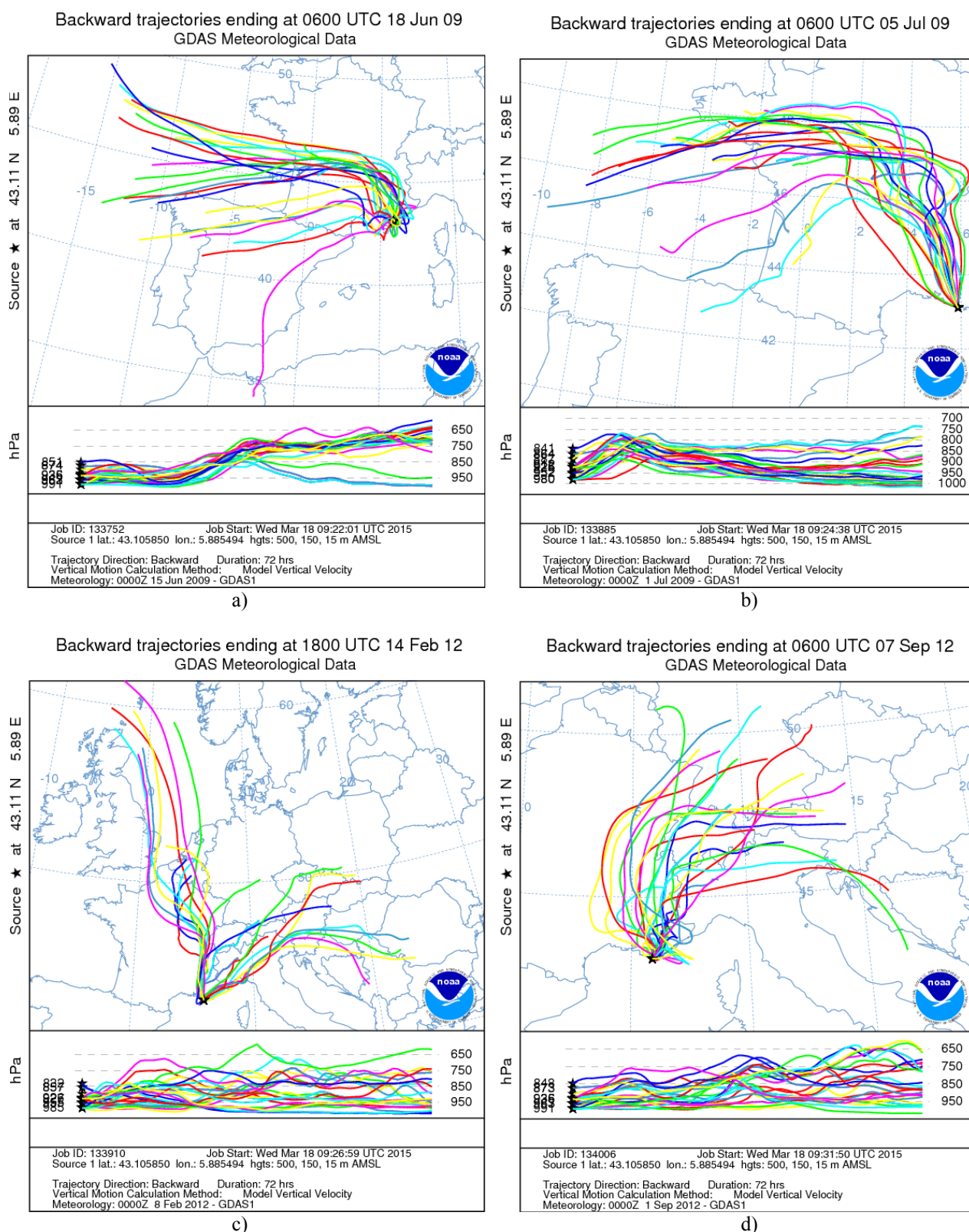
Fig. 8. days back-trajectories for 4 episode of high significant concentration of TGM (> 3 ng m^{-3}) observed for each years: a) 18th June 2009, 06:00 am; b) 05th July 2009, 06:00 am; c) 14th February 2012, 06:00 pm; d) 07th September 2012).

REFERENCES

Amos, H.M., Jacob, D.J., Holmes, C.D., Fisher, J.A., Wang, Q., Yantosca, R.M., Corbitt, E.S., Galarneau, E., Rutter, A.P., Gustin, M.S., Steffen, A., Schauer, J.J., Graydon, J.A., St Louis, V.L., Talbot, R.W., Edgerton, E.S., Zhang, Y. and Sunderland, E.M. (2012). Gas-Particle Partitioning of Atmospheric Hg(Ii) and Its Effect on Global Mercury Deposition. *Atmos. Chem. Phys.* 12: 591–603.

Amyot, M., Gill, G.A. and Morel, F.M.M. (1997). Production and Loss of Dissolved Gaseous Mercury in Coastal Seawater. *Environ. Sci. Technol.* 31: 3606–3611.

Angot, H., Barret, M., Magand, O., Ramonet, M. and Dommergue, A. (2014). A 2-Year Record of Atmospheric Mercury Species at a Background Southern Hemisphere Station on Amsterdam Island. *Atmos. Chem. Phys.* 14: 11461–11473.

Bethoux, J.P., Gentili, B., Morin, P., Nicolas, E., Pierre, C. and Ruiz-Pino, D. (1999). The Mediterranean Sea: A Miniature Ocean for Climatic and Environmental Studies and a Key for the Climatic Functioning of the North Atlantic. *Prog. Oceanogr.* 44: 131–146.

Ci, Z., Zhang, X. and Wang, Z. (2011). Elemental Mercury in Coastal Seawater of Yellow Sea, China: Temporal Variation and Airesea Exchange. *Atmos. Environ.* 45: 183–190.

Durrieu de Madron, X., Guieu, C., Sempéré, R., Conan, P., Cossa, D., D'Ortenzio, F., Estournel, C., Gazeau, F., Rabouille, C., Stemmann, L., Bonnet, S., Diaz, F., Koubbi, P., Radakovitch, O., Babin, M., Baklouti, M., Bancon-Montigny, C., Belviso, S., Bensoussan, N., Bonsang, B., Bouloubassi, I., Brunet, C., Cadiou, J.F., Carlotti, F., Chami, M., Charmasson, S., Charrière, B., Dachs, J., Doxaran, D., Dutay, J.C., Elbaz-Poulichet, F., Eléaume, M., Eyrolles, F., Fernandez, C., Fowler, S., Francour, P., Gaertner, J.C., Galzin, R., Gasparini, S., Ghiglione, J.F., Gonzalez, J.L., Goyet, C., Guidi, L., Guizien, K., Heimbürger, L.E., Jacquet, S.H.M., Jeffrey, W.H., Joux, F., Le Hir, P., Leblanc, K., Lefèvre, D., Lejeusne, C., Lemé, R., Loÿe-Pilot, M.D., Mallet, M., Méjanelle, L., Mélin, F., Mellon, C., Mérigot, B., Merle, P.L., Migon, C., Miller, W.L., Mortier, L., Mostajir, B., Mousseau, L., Moutin, T., Para, J., Pérez, T., Petrenko, A., Poggiale, J.C., Prieur, L., Pujo-Pay, M., Pulido, V., Raimbault, P., Rees, A.P., Ridame, C., Rontani, J.F., Ruiz Pino, D., Sicre, M.A., Taillandier, V., Tamburini, C., Tanaka, T., Taupier-Letage, I., Tedetti, M., Testor, P., Thébault, H., Thouvenin, B., Touratier, F., Tronczynski, J., Ulses, C., Van Wambeke, F., Vantrepotte, V., Vaz, S. and Verney, R. (2011). Marine Ecosystems' Responses to Climatic and Anthropogenic Forcings in the Mediterranean. *Prog. Oceanogr.* 91: 97–166.

Ferrara, R., Mazzolai, B., Lanzillotta, E., Nucaro, E. and Pirrone, N. (2000a). Temporal Trends in Gaseous Mercury Evasion from the Mediterranean Seawaters. *Sci. Total Environ.* 259: 183–190.

Ferrara, R., Mazzolai, B., Lanzillotta, E., Nucaro, E. and Pirrone, N. (2000b). Volcanoes as Emission Sources of Atmospheric Mercury in the Mediterranean Basin. *Sci. Total Environ.* 259: 115–121.

Fitzgerald, W.F., Lamborg, C.H. and Hammerschmidt, C.R. (2007). Marine Biogeochemical Cycling of Mercury. *Chem. Rev.* 107: 641–662.

Grell, G., Dudhia, J. and Stauffe, A.D. (1994). A Description of the Fifth Generation Penn State/Ncar Mesoscale Model (MM5). NCAR Tech. Note NCAR/TN-398 1 STR: 177 pp.

Hammerschmidt, C.R., Fitzgerald, W.F., Lamborg, C.H., Balcom, P.H. and Tseng, C.M. (2006). Biogeochemical Cycling of Methylmercury in Lakes and Tundra Watersheds of Arctic Alaska. *Environ. Sci. Technol.* 40: 1204–1211.

Kock, H.H., Bieber, E., Ebinghaus, R., Spain, T.G. and Thees, B. (2005). Comparison of Long-Term Trends and Seasonal Variations of Atmospheric Mercury Concentrations at the Two European Coastal Monitoring Stations Mace Head, Ireland, and Zingst, Germany. *Atmos. Environ.* 39: 7549–7556.

Kotnik, J., Sprovieri, F., Ogrinc, O., Horvat, M., Pirrone, N., (2013). Mercury in the Mediterranean, Part I : Spatial and Temporal Trends. *Environ. Sci. Pollut. Res.* 21: 4063–4080.

Lamborg, C.H., Fitzgerald, W.F., O'Donnell, J. and Torgersen, T. (2002). A Non-Steady State Box Model of Global-Scale Mercury Biogeochemistry with Interhemispheric Atmospheric Gradients. *Geochim. Cosmochim. Acta* 66: 1105–1118.

Lamborg, C.H., Hammerschmidt, C.R., Bowman, K.L., Swarr, G.J., Munson, K.M., Ohnemus, D.C., Lam, P.J., Heimburger, L.E., Rijkenberg, M.J.A. and Saito, M.A. (2014). A Global Ocean Inventory of Anthropogenic Mercury Based on Water Column Measurements. *Nature* 512: 65–83.

Lindberg, S., Bullock, R., Ebinghaus, R., Engstrom, D., Feng, X.B., Fitzgerald, W., Pirrone, N., Prestbo, E. and Seigneur, C. (2007). A Synthesis of Progress and Uncertainties in Attributing the Sources of Mercury in Deposition. *Ambio* 36: 19–32.

Munthe, J., Wangberg, I., Pirrone, N., Iverfeldt, A., Ferrara, R., Ebinghaus, R., Feng, X., Gardfeldt, K., Keeler, G., Lanzillotta, E., Lindberg, S.E., Lu, J., Mamane, Y., Prestbo, E., Schmolke, S., Schroeder, W.H., Sommar, J., Sprovieri, F., Stevens, R.K., Stratton, W., Tuncel, G. and Urba, A. (2001). Intercomparison of Methods for Sampling and Analysis of Atmospheric Mercury Species. *Atmos. Environ.* 35: 3007–3017.

Pirrone, N., Costa, P., Pacyna, J.M. and Ferrara, R. (2001). Mercury Emissions to the Atmosphere from Natural and

Anthropogenic Sources in the Mediterranean Region. *Atmos. Environ.* 35: 2997–3006.

Pirrone, N., Cinnirella, S., Feng, X., Finkelman, R.B., Friedli, H.R., Leaner, J., Mason, R., Mukherjee, A.B., Stracher, G.B., Streets, D.G. and Telmer, K. (2010). Global Mercury Emissions to the Atmosphere from Anthropogenic and Natural Sources. *Atmos. Chem. Phys.* 10: 5951–5964.

Poissant, L., Zhang, H.H., Canario, J. and Constant, P. (2008). Critical Review of Mercury Fates and Contamination in the Arctic Tundra Ecosystem. *Sci. Total Environ.* 400: 173–211.

Selin, N.E., Jacob, D.J., Park, R.J., Yantosca, R.M., Strode, S., Jaegle, L. and Jaffe, D. (2007). Chemical Cycling and Deposition of Atmospheric Mercury: Global Constraints from Observations. *J. Geophys. Res.* 112: D02308.

Slemr, F., Brunke, E.-G., Ebinghaus, R., Temme, C., Munthe, J., Wängberg, I., Schroeder, W., Steffen, A. and Berg, T. (2003). Worldwide Trend of Atmospheric Mercury since 1977. *Geophys. Res. Lett.* 30: 1516.

Slemr, F., Brunke, E.G., Ebinghaus, R. and Kuss, J. (2011). Worldwide Trend of Atmospheric Mercury Since 1995. *Atmos. Chem. Phys.* 11: 4779–4787.

Urba, A., Kvietkus, K., Sakalys, J., Xiao, Z. and Lindqvist, O. (1995). A New Sensitive and Portable Mercury-Vapor Analyzer Gardis-1a. *Water Air Soil Pollut.* 80: 1305–1309.

Wangberg, I., Munthe, J., Pirrone, N., Iverfeldt, A., Bahlman, E., Costa, P., Ebinghaus, R., Feng, X., Ferrara, R., Gardfeldt, K., Kock, H., Lanzillotta, E., Mamane, Y., Mas, F., Melamed, E., Osnat, Y., Prestbo, E., Sommar, J., Schmolke, S., Spain, G., Sprovieri, F. and Tuncel, G. (2001). Atmospheric Mercury Distribution in Northern Europe and in the Mediterranean Region. *Atmos. Environ.* 35: 3019–3025.

Wangberg, I., Munthe, J., Amouroux, D., Andersson, M.E., Fajon, V., Ferrara, R., Gardfeldt, K., Horvat, M., Mamane, Y., Melamed, E., Monperrus, M., Ogrinc, N., Yossef, O., Pirrone, N., Sommar, J. and Sprovieri, F. (2008). Atmospheric Mercury at Mediterranean Coastal Stations. *Environ. Fluid Mech.* 8: 101–116.